Magnetic Fields Across the Hertzsprung-Russell Diagram
ASP Conference Series, Vol. , 2001
G. Mathys, S. Solanki and D. T. Wickramasinghe

Observations of Solar Coronal Magnetic Fields

Stephen M. White

Department of Astronomy, University of Maryland, College Park, MD 20742, USA

Abstract. This review discusses methods for determining solar coronal magnetic fields, with an emphasis on radio measurements of field strengths in solar active regions.

1. Introduction

Coronal magnetic fields are believed to play a crucial role in several major unsolved mysteries of solar physics, including coronal heating, solar flares and coronal mass ejections. However, measurement of coronal magnetic fields is not as routine as measurement of solar photospheric fields. The measurement of fields throughout the coronal volume is an intrinsically more difficult problem since it requires three–dimensional information, whereas photospheric fields are measured on a two–dimensional surface. The techniques used to measure magnetic fields in the photosphere rely on Zeeman splitting and Stokes profile measurements and are not as effective in the solar corona, since lines formed at coronal temperatures are intrinsically broader and are scarce in the infrared where Zeeman splitting is (relatively) large. When suitable lines exist in the infrared and optical regimes (e.g., Judge 1998, Kuhn et al. 1999, Lin et al. 2000), they can only be used for observations above the limb because of the strong photospheric flux which contaminates the spectra against the solar disk. Coronal lines are prevalent at X–ray and EUV wavelengths and can be used to observe regions on the solar disk, but polarimetry is more difficult at these wavelengths and Zeeman splitting is only a small fraction of the natural widths of the lines.

As the superb images from the EUV telescopes on the SOHO and TRACE satellites have shown, EUV and X–ray wavelengths are ideal for tracing magnetic field lines in the solar corona. This is because the line emission processes responsible for coronal lines are proportional to the square of the number density, and thus are very sensitive to density contrasts. In a strongly magnetized plasma the inhibition of transport perpendicular to the magnetic field naturally results in such strong density contrasts, but only a subset of the coronal field lines is illuminated by this process.

In principal, one can determine the coronal magnetic field distribution from the photospheric magnetic field distribution under certain assumptions. Given a complete measurement of the vector magnetic field $\mathbf{B}$ at a surface, one can solve a boundary value problem for the distribution of $\mathbf{B}$ throughout the volume above the boundary using the nonlinear equations $(\nabla \times \mathbf{B}) \times \mathbf{B} = 0$ and $\nabla \cdot \mathbf{B} = 0$. Here the assumption that the coronal field is force–free has been made, i.e.,

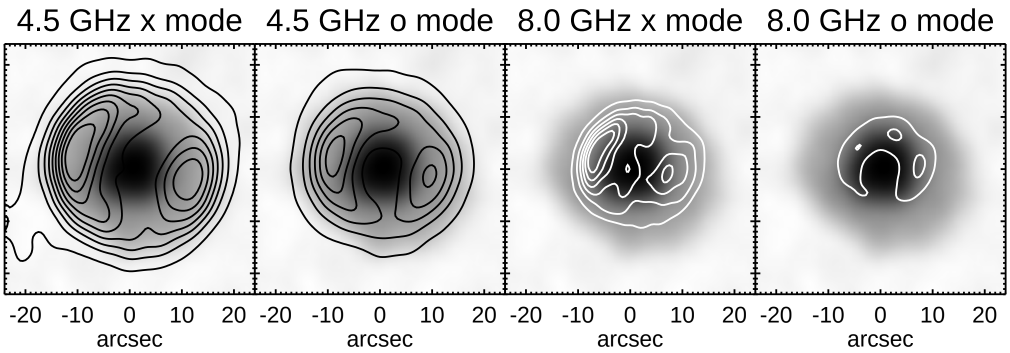

Figure 1. Radio contours (at two frequencies in each sense of circular polarization) plotted over a white light image of a sunspot for a particularly simple spot observed close to disk center with the Very Large Array on 1994 October 15. Contours are plotted at brightness temperatures of 1, 3, 5, 7, ... $\times\ 10^5$ K. The radio emission is low over the center of the spot where we are looking nearly parallel to the magnetic field direction in the corona and the opacity is low, whereas at the outer edge of the spot the opacity is high because θ is larger and optically thick radio emission at coronal temperatures is observed.

any currents present in the corona must flow along field lines. The system of equations plus a boundary measurement set constitutes a mixed elliptic–hyperbolic boundary value problem which has proven remarkably difficult to solve (Gary 1989, McClymont & Mikić 1994, Amari et al. 1999). One can write generally $\nabla \times \mathbf{B} = \alpha(\mathbf{r})\mathbf{B}$ and solve for the scalar $\alpha(\mathbf{r})$, which is constant along field lines since $\mathbf{B} \cdot \nabla\alpha(\mathbf{r}) = 0$. Common approximations are the potential approximation ($\nabla \times \mathbf{B} = 0$, $\mathbf{B} = \nabla\phi$, where ϕ is a scalar potential), only valid if no currents are present, and the "linear force–free solution" (α is a constant everywhere). Unfortunately the observations indicate that α is not a constant in a given coronal region.

Numerical methods for solving the full nonlinear force–free equations have been developed. Relaxation techniques have had considerable success at producing an accurate solution to the equations, as judged by comparisons with observed magnetic field lines (Jiao, McClymont, & Mikić 1997) and measured coronal magnetic field strengths (Lee et al. 1998), but there are some limitations: the direction of the transverse component of the magnetic field in the corona cannot be determined unambiguously (to within 180°); errors in measurements of the photospheric magnetic field affect the reconstruction of the coronal field; and the photospheric values of α may not be appropriate in the corona since the photosphere is not force–free (Metcalf et al. 1995). In the future measurements of the chromospheric magnetic field may avoid this latter difficulty.

2. Radio Measurements of Coronal Magnetic Field Strengths

Radio observations measure coronal magnetic field strengths using gyroresonance emission. They can presently be used for field strengths in excess of several hundred Gauss. The mechanism involves a resonance between electromagnetic waves and electrons spiralling along magnetic field lines at the electron gyrofrequency, $f_B = 2.80 \times 10^6\ B$ Hz, where B is measured in G. This resonance produces strong coupling between electrons and radiation at low harmonics of the electron gyrofrequency ($f = sf_B$ where s = 1, 2, 3, 4). The properties of the mechanism are very well understood (e.g., Zlotnik 1968; White & Kundu 1997): (i) The two natural electromagnetic modes of the plasma are circularly polarized under most conditions: the x mode, which rotates in the same sense as the electron gyrates about the field, interacts more strongly than the o mode which has the opposite sense of rotation. The o mode opacity is always at least an order of magnitude smaller than the x mode opacity. (ii) The gyroresonance opacity at harmonic s is $\propto\ N_e\,(s^2\,\sin^2\theta\,T_e/m_ec^2)^{s-1}$, where θ is the angle between the line of sight and the magnetic field direction in the source, N_e the electron density and T_e is the temperature. The opacity drops sharply towards small θ (**B** parallel to the line of sight) in both modes. (iii) For typical coronal conditions, the x mode is optically thick ($\tau \geq 1$) in the $s = 2$ and 3 layers over a broad range of angles θ. The o mode is optically thick over most of the s = 2 layer, and may be at least marginally optically thick over a small portion of the $s = 3$ layer where θ is large. Harmonics greater than $s = 4$ do not have any significant optical depth in the quiet solar corona, although there may be x mode emission from the 4th harmonic if the temperature is high (Lee et al. 1997). (iv) For each increase of s by 1, the opacity in a given mode at a given angle drops by slightly more than 2 orders of magnitude. This is largely due to the $(T_e/mc^2)^s$ dependence of the opacity. The importance of this large change in opacity from one layer to the next is that a given harmonic layer is likely to be either optically thick over a wide range of angles θ, or else optically thin everywhere. Density has much less influence on the opacity than the harmonic number. B typically varies by less than 2% across a resonant layer.

Because radio wavelengths are in the Rayleigh–Jeans limit (i.e., well to the long wavelength side of the thermal peak in the electromagnetic spectrum), the radio brightness temperature on the sky is proportional to the temperature of the source: $T_B = (1 - e^{-\tau})T_e$, where τ is the optical depth through the source. In particular, wherever the atmosphere is optically thick to radio emission, the observed radio brightness temperature is the actual temperature of the electrons which produce the emission. This fact provides a useful tool: any feature which is observed to have a coronal brightness temperature is therefore optically thick. Bremsstrahlung from the hot dense plasma in loops above active regions is optically thick only at the lower radio frequencies (below 3 GHz). A technique which exploits both gyroresonance and bremsstrahlung emission to derive the magnetic field, using EUV data to “remove” the bremsstrahlung contribution, has been developed by Brosius et al. (1997).

When “decoding” observations of gyroresonance emission in terms of coronal magnetic fields, we can regard any source above 3 GHz which has a coronal brightness temperature or a high degree of circular polarization as a gyroresonance source. It is helpful to think in terms of the surfaces of constant magnetic field strength (“isogauss”) above an active region. At a given frequency f, gyroresonance opacity is only significant in the isogauss layers along the line of sight at which $f_B = f/s$, s = 1,2,3,... When we look down on an active region from above, we see down to the highest isogauss layer which is optically thick in

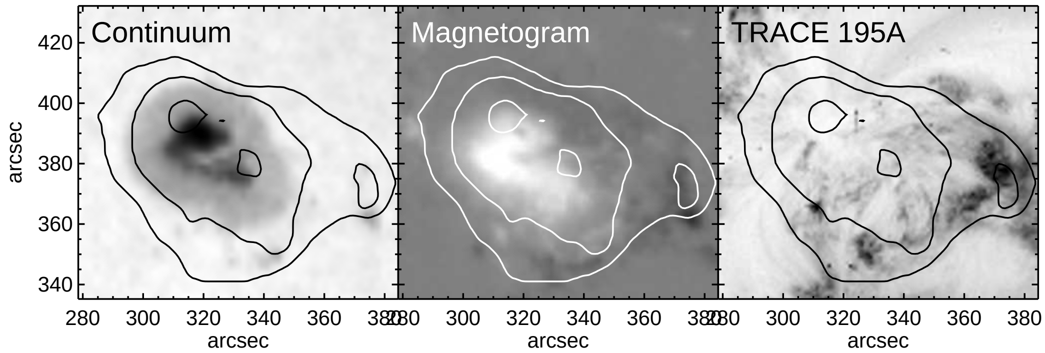

Figure 2. Contours of magnetic field strength at the base of the corona plotted on white light (left), magnetogram (middle) and TRACE 195 Å Fe XII (right) images of a sunspot observed on 1999 May 13. The coronal contours are plotted at 500, 900 and 1700 G, corresponding to the radio images at 4.5, 8.0 and 15.0 GHz used to construct the coronal magnetogram.

the corona. This will generally be the $s = 3$ layer in the sense of circular polarization corresponding to the x mode and the $s = 2$ layer in the o mode, e.g., the 600 G layer in the x mode and 900 G in the o mode at 5 GHz. For a region on the disk, θ, and therefore opacity, will be largest at the outer boundary of an isogauss layer: thus the outer boundary of the optically thick radio source should indicate where the isogauss surface drops below the corona into the chromosphere. This property allows us straightforwardly to measure the magnetic field strength at the base of the corona (Figure 2). In the Sun's atmosphere different radio wavelengths are optically thick at different heights and thus all layers can be studied by making images at many frequencies across a broad frequency range. This gives us the three–dimensional information necessary to study the coronal field, whereas an optically thin diagnostic necessarily integrates over all emission along the line of sight and no discrimination for depth is possible.

3. Properties of Coronal Magnetic Field Strengths

A common argument applied to coronal magnetic field strengths is as follows: magnetic flux in the (high–β) solar photosphere tends to be concentrated in small regions of intense (kG) field strength. As this flux rises into the low–β solar corona it will expand laterally, thus diminishing the strength of the field. This argument is the basis for the wide–spread belief that coronal magnetic fields are much weaker than the fields measured in the photosphere. The argument appears to be valid for the quiet–Sun fields concentrated in small flux tubes in the cell network: if these fields reached the solar corona with strengths of order of hundreds of G or more, we would see clear signatures in radio images of the Sun in the form of features over the network at coronal temperatures. Such signatures are not seen (e.g., Gary et al. 1990).

On the other hand, the argument does not apply to active regions fields. Field strengths of 2000 G or more can be found in the corona, particularly over large sunspots (Shibasaki et al. 1994): in active regions there is so much flux that there is little field–free volume to expand into, and so field strength declines much less rapidly with height than simple models tend to predict (Akhmedov et al. 1982). For example, in Figure 2 the maximum line–of–sight field in the photosphere is not much more than 2000 G, yet coronal fields of 1800 G are found to be present. The recent coronal line measurements above active regions at the limb agree with this conclusion (Lin et al. 2000), as does the fact that loop width measurements find that coronal loops tend to have constant widths, rather than showing expansion at greater heights (McClymont & Mikić 1994, Klimchuk 2000). Since active stars are also inferred to have large filling factors of strong magnetic field strength at the stellar photosphere, the same argument suggests that active stellar coronae should have strong fields throughout (but see the discussion in White et al. 1994).

One interesting aspect of coronal magnetic field observations is that they indicate that field strengths do not change nearly as rapidly as do, for example, coronal densities. EUV images show coronal loops filling and emptying continually on timescales as short as a minute or less, and this has led to the picture of the corona as a very dynamic region. However, if we were to image the coronal magnetic field strength in the same way that EUV images show density, we would have a very different picture: field strengths change much more slowly. This is consistent with the much longer inductive timescales associated with changing magnetic fields rooted in the solar interior and the observed timescale of magnetic evolution at the photosphere.

References

Akhmedov, S. B., Gelfreikh, G., Bogod, V., et al. 1982, Solar Phys., 79, 41

Amari, T., Boulmezaoud, T. Z., & Mikić, Z. 1999, A&A, 350, 1051

Brosius, J. W., Davila, J., Thomas, R., & White, S. 1997, ApJ, 488, 488

Gary, D. E., Zirin, H. & Wang, H. 1990, ApJ, 355, 321

Gary, G. A. 1989, ApJS, 69, 323

Jiao, L., McClymont, A. N., & Mikić, Z. 1997, Solar Phys., 174, 311

Judge, P. G. 1998, ApJ, 500, 1009

Klimchuk, J. A. 2000, Solar Phys., 193, 53

Kuhn, J. R., MacQueen, R. M., Streete, J., et al. 1999, ApJ, 521, 478

Lee, J., McClymont, A., Mikić, Z., White, S., & Kundu, M. 1998, ApJ, 501, 853

Lee, J., White, S., Gopalswamy, N., & Kundu, M. 1997, Solar Phys., 174, 175

Lin, H., Penn, M. J., & Tomczyk, S. 2000, ApJL, 541, L83

McClymont, A. N. & Mikić, Z. 1994, ApJ, 422, 899

Metcalf, T. R., Jiao, L., McClymont, A. N., et al. 1995, ApJ, 439, 474

Shibasaki, K., Enome, S., Nakajima, H., and 13 others, 1994, PASJ, 46, L17

White, S. M., & Kundu, M. R. 1997, Solar Phys., 174, 31

White, S. M., Lim, J., & Kundu, M. R. 1994, ApJ, 422, 293

Zlotnik, E. Ya. 1968, Sov. Astron. J. 12, 245